Published online 11 March 2011 Nucleic Acids Research, 2011, Vol. 39, No. 13 5633–5646
doi:10.1093/nar/gkr083

An essential role for trimethylguanosine RNA caps in *Saccharomyces cerevisiae* meiosis and their requirement for splicing of *SAE3* and *PCH2* meiotic pre-mRNAs

Zhicheng R. Qiu[1], Stewart Shuman[1,*] and Beate Schwer[2,*]

[1]Molecular Biology Program, Sloan-Kettering Institute and [2]Department of Microbiology and Immunology, Weill Cornell Medical College, New York, NY 10065 USA

Received January 7, 2011; Revised January 28, 2011; Accepted February 2, 2011

ABSTRACT

Tgs1 is the enzyme that converts m^7G RNA caps to the 2,2,7-trimethylguanosine (TMG) caps characteristic of spliceosomal snRNAs. Fungi grow vegetatively without TMG caps, thereby raising the question of what cellular transactions, if any, are TMG cap-dependent. Here, we report that *Saccharomyces cerevisiae* Tgs1 methyltransferase activity is essential for meiosis. *tgs1Δ* cells are specifically defective in splicing *PCH2* and *SAE3* meiotic pre-mRNAs. The TMG requirement for *SAE3* splicing is alleviated by two intron mutations: a UAUUAAC to UACUAAC change that restores a consensus branchpoint and disruption of a stem–loop encompassing the branchpoint. The TMG requirement for *PCH2* splicing is alleviated by a CA CUAAC to UACUAAC change restoring a consensus branchpoint and by shortening the *PCH2* 5′ exon. Placing the *SAE3* and *PCH2* introns within a *HIS3* reporter confers Tgs1-dependent histidine prototrophy, signifying that the respective introns are portable determinants of TMG-dependent gene expression. Analysis of *in vitro* splicing in extracts of *TGS1* versus *tgs1Δ* cells showed that *SAE3* intron removal was enfeebled without TMG caps, whereas splicing of *ACT1* was unaffected. Our findings illuminate a new mode of tunable splicing, a reliance on TMG caps for an essential developmental RNA transaction, and three genetically distinct meiotic splicing regulons in budding yeast.

INTRODUCTION

Hypermethylated 2,2,7-trimethylguanosine (TMG) cap structures are characteristic of the small nuclear RNAs that program mRNA splicing (U1, U2, U4 and U5) (1). TMG is formed from m^7G caps by the enzyme Tgs1 (2), which catalyzes two successive methyl transfer reactions from AdoMet to the N2 atom of 7-methylguanosine (3–8). Whereas guanylate caps are essential in all eukarya that have been examined genetically, the TMG cap is conspicuously not. A *tgs1Δ* mutant of fission yeast *Schizosaccharomyces pombe* grows normally (5). The *tgs1Δ* mutation of budding yeast *S. cerevisiae* causes a growth defect at cold temperatures, although *tgs1Δ* cells grow as well as *TGS1* cells at 34°C (2,6). The *tgs1Δ* mutants of budding and fission yeast lack any detectable TMG caps on their U1, U2, U4 and U5 small nuclear RNAs (snRNAs) and small nucleolar RNAs (snoRNAs) (2,5), signifying that there is no Tgs1-independent route to generate TMG caps *in vivo*. Tgs1 depletion by RNAi in HeLa cells, which reduced Tgs1 protein levels to below the limit of detection, had no effect on cell growth (9). On the other hand, TMG synthesis plays an essential role during animal development, whereby mutations in the *Drosophila* Tgs1 methyltransferase active site caused lethality at the early pupal stage, which correlated with depletion of TMG-containing RNAs (10).

The initially surprising conclusion that fungi and human somatic cells grow in the absence of Tgs1 suggested that there might be backup mechanisms to ensure the function of the many essential TMG-capped RNAs when the TMG modification is missing. This idea was confirmed via synthetic enhancement genetics in budding yeast (6,11), which highlighted a redundant role of the

*To whom correspondence should be addressed. Email: s-shuman@ski.mskcc.org
Correspondence may also be addressed to Beate Schwer. Email: bschwer@med.cornell.edu

TMG cap in spliceosome assembly. The output of the genome-wide screen reported in Hausmann *et al.* (6) for mutational enhancement of *tgs1Δ* was highly enriched in proteins implicated in U1 and U2 snRNP function during pre-mRNA splicing. The two strongest interactors with Tgs1, resulting in synthetic lethality, were Mud2 and Nam8. Nam8 is an RNA-binding component of the U1 snRNP and is present in the commitment complex of U1 snRNP at the 5′ splice site (12,13). Nam8 is a putative homolog of the mammalian RNA-binding protein and splicing factor TIA-1 (14–16). Mud2, the yeast homolog of metazoan splicing factor U2AF65, interacts with the pre-mRNA/U1snRNP commitment complex in a manner that depends on the branchpoint sequence of the intron; Mud2 is proposed to facilitate subsequent recruitment of the U2 snRNP (17,18). Synthetic interactions of Tgs1 with other splicing factors (Brr1, Lea1, Ist3, Mud1, Isy1, Cwc21 and Bud13) fortify the case for a genetically redundant role of the TMG cap in mitotically growing yeast (6). This raises the question of what cellular transactions, if any, are TMG cap-dependent *per se*.

Among the vegetatively optional yeast splicing factors in the Tgs1 genetic 'neighborhood', Nam8 stands out because it is strictly essential for meiosis. During sporulation, Nam8 promotes the splicing of specific mRNAs that encode proteins required for meiotic recombination and cell division (19–22). Nam8-dependent splicing of four meiotic mRNAs—*AMA1*, *MER2*, *MER3* and *SPO22*—is activated by the meiotic splicing regulator Mer1 (16,23–25), which is produced only in meiotic cells under the control of the meiotic transcription factor Ime1 (26). Mer1 activates splicing by binding to an intronic splicing enhancer sequence (5′-AYACCCUY-3′) present in the *AMA1*, *MER2, MER3* and *SPO22* pre-mRNAs (16,20). Mer1 bound to the intronic enhancer is thought to promote assembly of the U1 and U2 snRNPs on the pre-mRNA. We recently showed that Nam8 plays a distinct Mer1-independent role in splicing of the *PCH2* meiotic pre-mRNA, thereby establishing the existence of two genetically distinct meiotic splicing regulons (16). Transcripts subject to Mer1 and Nam8 splicing regulation have either suboptimal 5′ splice sites, suboptimal branchpoints or a large 5′ exon that apparently dictate their reliance on otherwise inessential splicing factors (16,21,27,28).

Here, we queried whether Tgs1 and TMG caps might also be specifically required for RNA transactions during meiosis. Previously, a screen of the yeast single-gene deletion library for defects in sporulation and meiosis had identified *YPL157W* (*TGS1*) as a sporulation gene (29), but the connection between Tgs1 and cap trimethylation had not yet been made when this screen was conducted and no insights were made to how *YPL157W* might act during meiotic development. We now report that Tgs1 and, most importantly, its methyltransferase activity are required for sporulation, because TMG caps promote splicing of a novel meiotic pre-mRNA regulon. By evaluating the splicing of the known meiosis-specific pre-mRNAs (16,30–34) in wild-type and *tgs1Δ* yeast diploids during attempted sporulation, we discovered that Tgs1 is required for efficient splicing of two meiotic mRNAs that lack a Mer1-binding site: *SAE3* and *PCH2*. In each case, we identified the distinctive features of the pre-mRNA that dictate Tgs1-dependence *in vivo*. Analysis of *in vitro* splicing in extracts of *TGS1* versus *tgs1Δ* cells showed that *SAE3* intron removal was enfeebled selectively absent TMG caps, while splicing of the *ACT1* and *U3* introns was unaffected. Our findings highlight new complexity in regulated splicing in yeast and the context-dependent reliance on TMG caps for an essential RNA transaction.

MATERIALS AND METHODS

Yeast strains

The meiosis/sporulation experiments were carried out with isogenic diploids in the SK1 background. To generate *tgs1Δ* diploids, haploid derivatives of the SK1 strain, SKY163 (*MAT*a *ho::LYS2 lys2 ura3 leu2::hisG*) and SKY164 (*MAT*α *ho::LYS2 lys2 ura3 leu2::hisG*) were used. In brief, DNA segments encompassing the *tgs1::kanMX* and *tgs1::natMX* disruption cassettes were generated by polymerase chain reaction (PCR) amplification of genomic DNA from the respective *tgs1Δ* yeast strains (6) using primers flanking the cassette. One of the PCR products (*tgs1::kanMX*) was introduced into SKY163 and geneticin-resistant integrants were selected. SKY164 was transformed with a *tgs1::natMX* deletion cassette and nourseothricin-resistant *natMX* integrants were selected. The targeted insertions were confirmed by diagnostic Southern blotting. The SKY haploids were then mated and homozygous *tgs1Δ* diploids were selected on yeast peptone dextrose (YPD) agar containing 100 μg/ml nourseothricin and 150 μg/ml geneticin.

Integration of *TGS1* and *tgs1-D126A* at the *leu2* locus of SKY *tgs1Δ* strains was performed as follows. To generate the targeting cassettes, DNA fragments (1.5 kb) spanning the *TGS1* and *tgs1-D126A* genes under the control of the native *TGS1* promoter were excised from pUN100-based plasmids (6) and inserted into the polylinker of the integrative pRS305 (*LEU2*) vector. The resulting plasmids were restricted with EcoRV within the *LEU2* gene and the linearized plasmids were transformed into the SKY haploids *tgs1Δ::kanMX* and *tgs1Δ::natMX*. Leu^+ transformants were selected and diagnostic Southern blotting was used to confirm the correct integrations of the *LEU2* plasmid at *leu2*. The corresponding haploids were then mated and *tgs1Δ leu2::[LEU2 TGS1]* and *tgs1Δ leu2::[LEU2 tgs1-D126A]* diploids were selected.

Sporulation and analysis of meiotic RNA splicing

Single colonies of diploid yeast strains were patched on agar plates with glycerol as the carbon source for at least 6 h to select for cells with healthy mitochondria. Cells were streaked on YPD agar plates and incubated for 3 days at 30°C. Single colonies were then inoculated into YPD liquid medium and grown at 30°C to stationary phase (A_{600} of 6–8). Aliquots were inoculated into 12.5 ml of presporulation medium [0.5% yeast extract, 1% peptone, 0.67% yeast nitrogen base (without amino acids), 1% potassium acetate, 0.05 M potassium biphthalate (pH 5.5), 0.002% antifoam 204] to attain an A_{600} of 0.8. The cultures were incubated for 7 h at 30°C and added to 100 ml of fresh presporulation medium to attain an A_{600} of 0.025 (wild-type cells) or 0.1 (*tgs1Δ* cells). These cultures were incubated for 16 h until A_{600} reached ~3.0. The cells were harvested by centrifugation, washed twice with sporulation medium (2% potassium acetate, 0.001% polypropylene glycol) and then resuspended in sporulation medium at A_{600} of 6. Aliquots were withdrawn from synchronous meiotic cultures at 6, 8, 10, 12, 14 and 24 h post transfer to sporulation medium. The cells were fixed in an equal volume of 100% ethanol and then examined by light microscopy (100× magnification) to assess the abundance of 4-spore asci. Two-hundred cells from each sample were scored. The extents of sporulation (% asci) are plotted as a function of time in Figure 1. Each datum is the average of three separate experiments ± SEM.

For analysis of meiotic RNA, 2-ml aliquots of the cultures were withdrawn immediately prior to transfer to sporulation medium and at 4 h and 8 h post-transfer to sporulation medium. Cells were harvested by centrifugation and RNA was extracted from the cells by using the MasterPure Yeast RNA Purification Kit (Epicentre BioTechnologies). The DNase digestion step in the RNA purification protocol was modified such that the samples were incubated for 1 h with 20 U of RNase-free DNase I (New England Biolabs) to eliminate genomic DNA. First-strand cDNA was synthesized in reaction mixtures containing 10 ng/μl total RNA, 25 ng/μl oligo$(dT)_{12–18}$ primer, 10 U/μl SuperScript II (Invitrogen), 1X First Strand Buffer, 10 mM dithiothreitol (DTT) and 0.5 mM deoxynucleotide triphosphates (dNTPs). RNA, dNTPs and primers were preincubated for 5 min at 65°C before quick chilling on ice. DTT and First Strand Buffer were added, and the mixture was incubated at 42°C for 2 min. Finally, reverse transcriptase was added and the reaction mixture was incubated at 42°C for 50 min and then at 70°C for 15 min. The cDNAs for meiotic transcripts were then PCR-amplified in 25 μl reaction mixtures containing 1X native *Pfu* buffer, 0.2 mM dNTPs, 0.8 μM gene-specific sense strand primer and 0.8 μM 5′-^{32}P-labeled gene-specific antisense strand primer (16), 0.05 U/μl *Pfu* DNA Polymerase (Agilent Technologies) and 2 μl of each cDNA sample. The PCR cycles (n = 31) entailed incubations at 94°C for 30 s, 55°C for 90 s and 72°C for 2 min. The reverse transcriptase (RT)–PCR products were analyzed by electrophoresis through 2% native agarose gels. After electrophoresis, the gels were stained with ethidium bromide and then dried under vacuum on DEAE paper. The ^{32}P-labeled PCR products were visualized by autoradiography and quantified by scanning with a Fuji BAS-2500 imager.

Assay of splicing of meiotic RNAs in vegetative cells

A haploid 'wild-type' *TGS1* yeast strain (*MAT*a *TGS1 leu2Δ ura3Δ*), derived from S288c, and a *tgs1::natMX* variant thereof (6) were transformed with plasmids expressing *MER1*, *SPO22*, *SAE3* or *PCH2*. The expression plasmids were as follows. pYX212-MER1 (2*μ URA3 TPI1-MER1*) has the *MER1* open reading frame under the transcriptional control of the yeast *TPI1* promoter. pRS425TPI-SPO22 (2*μ LEU2 TPI1-SPO22*) carries the intron-containing *SPO22* gene driven by the *TPI1* promoter. pRS425-PCH2 (2*μ LEU2 PCH2*) bears the intron-containing *PCH2* gene (from 540 bp upstream of the translation start codon to 265 bp downstream of the stop codon) under the control of its native promoter. pRS425-SAE3 (2*μ LEU2 SAE3*) includes the intron-containing *SAE3* gene (from 370-bp upstream of the start codon to 255-bp downstream of the stop codon) under the control of its native promoter. *SAE3* and *PCH2* intron mutants (see Figures 4 and 8) were generated by two-stage overlap extension PCR with mutagenic primers; the mutated *SAE3* and *PCH2* DNAs were inserted into pRS425. The inserts of all plasmid clones were sequenced to exclude the acquisition of unwanted mutations during amplification and cloning.

The haploid plasmid-bearing yeast strains were grown in SD-(Ura^-Leu^-) liquid medium at 30°C until A_{600} reached 2–4. Cells were harvested by centrifugation from 2-ml aliquots of the cultures. RNA extractions and RT–PCR were performed as described above, with exceptions as follows: (i) cDNA synthesis was primed with

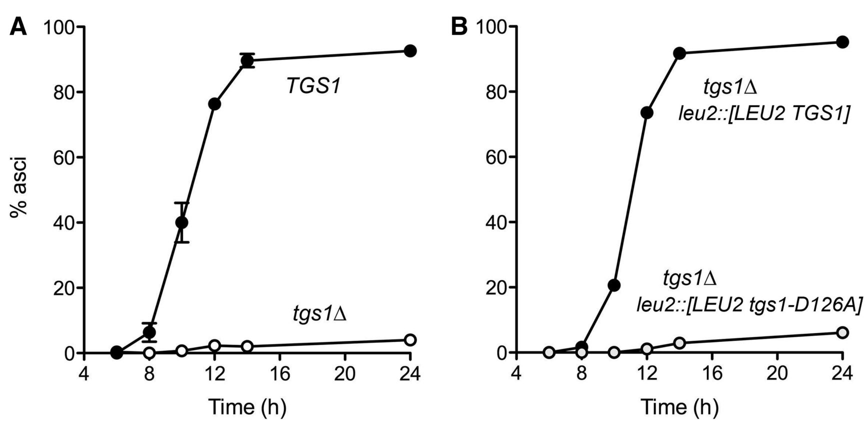

Figure 1. Tgs1 is required for yeast sporulation. (**A**) Wild-type and *tgs1Δ* diploids were examined by light microscopy at the indicated times after transfer to sporulation medium. (**B**) *tgs1Δ* diploids with wild-type yeast *TGS1* or a methyltransferase-defective mutant *tgs1-D126A* integrated at the chromosomal *LEU2* locus were examined by light microcopy at the indicated times after transfer to sporulation medium. The percentages of the cell population comprising 4-spore asci are plotted as a function of time. Each datum is the average of three independent experiments ± SEM.

0.1 μM gene-specific antisense primers (16) instead of oligo(dT)$_{12–18}$; (ii) the numbers of PCR cycles for amplification of *MER2, PCH2, SAE3* and *SPO22* cDNAs were 28, 27, 29 and 25, respectively; (iii) the PCR reactions were quenched by adding ethylenediaminetetraacetic acid (EDTA) and sodium dodecyl sulfate (SDS) to a final concentrations of 12.5 mM and 3.3%, respectively; and (iv) the ^{32}P-labeled PCR products were analyzed by electrophoresis through native 5% polyacrylamide gels containing 90 mM Tris-borate, 1.2 mM EDTA.

Yeast whole-cell extracts and *in vitro* splicing

Strains used for extract preparation were BJ2168 (*MATa leu2 trp1 ura3-52 prp1-1122 pep4-3 prc1-407 gal2*) and BJ-Δtgs1, a derivative of BJ2168 in which the *TGS1* locus was replaced by the *tgs1::natMX* deletion cassette (6). Cultures (6 l) were grown in YPD medium at 30°C until A_{600} reached 2.0–2.5. Whole-cell extracts were prepared as described (42). ^{32}P-GMP-labeled intron-containing precursor RNAs were transcribed from linearized plasmid templates by T7 RNA polymerase and purified by gel-filtration through Sepharose CL-6B (42). Splicing reaction mixtures containing 40% (v/v) extract, 60 mM potassium phosphate (pH 7.0), 2 mM adenosine triphosphate (ATP), 2 mM $MgCl_2$, 3% (w/v) PEG8000 and 1 nM precursor RNA were incubated at 28°C. The reaction products were analyzed by electrophoresis through a 6% polyacrylamide gel containing 7 M urea in TBE. The labeled RNAs were visualized by autoradiography of the dried gel and quantified by scanning with a Typhoon phosphorimager (Molecular Dynamics). The splicing efficiencies [spliced/(spliced + unspliced)] × 100 were calculated after normalizing the values for the ^{32}P-GMP content in the two RNA species.

HIS3 reporter assay for *SAE3* and *PCH2* intron splicing

To generate integration cassettes for the *HIS3* reporter genes, a 1-bp genomic DNA fragment spanning the *HIS3* ORF plus 297 and 20 bp of upstream and downstream sequences was amplified by PCR using primers His3-F and His3-R (Supplementary Table S1) and inserted in between the XmaI and PstI sites in pUC19. To insert the *SAE3* intron (or the mutated versions) at nucleotide position +48 in the *HIS3* ORF, we individually amplified the *HIS3*-5′ gene fragment (345 bp) with primers HIS3-F and SAE3-exon1R (Supplementary Table S1) and the *HIS3*-3′ gene fragment (635 bp) with primers HIS3-R and SAE3-exon2F (Supplementary Table S1). The *SAE3*, *SAE3-BP* and *SAE3Δhp* introns were amplified by PCR with primers SAE3-intronF and SAE3-intronR. The exon and intron DNA fragments with overlapping terminal sequences were then assembled into intron-punctuated *HIS3* cassettes by overlap-extension PCR and the cassettes were inserted into pUC19 plasmids. Using the same strategy and primers listed in Supplementary Table S1, the *PCH2* intron was inserted to generate *HIS3-[PCH2]-5′*. The pUC19-based plasmids harboring *HIS3-[PCH2]* and *HIS3-[PCH2-BP]* (in which the *PCH2* intron is inserted at position 430 within the *HIS3* ORF) were described previously (16). The cassettes were excised with SmaI and PstI and transformed into *tgs1Δ::natR* p360-TGS1 (*URA3 TGS1*) cells and isogenic wild-type cells (harboring a *URA3* plasmid) that were histidine-auxotrophs. His$^+$Ura$^+$ transformants were selected and analyzed for integration of the respective cassettes at the *HIS3* locus by diagnostic Southern blotting and by sequencing of DNA fragments PCR-amplified from genomic DNA using primers flanking the *HIS3* gene. The cells were then streaked to medium containing 5-FOA (and histidine) to select for cells that had lost the *URA3* plasmids. Individual colonies were patched to YPD agar. Cells were grown in liquid YPD medium until the cultures attained A_{600} of 0.7–0.9. The cultures were diluted in water to A_{600} of 0.01. Serial 10-fold dilutions were prepared and aliquots (3 μl) of each were spotted in parallel on SD agar medium with or without histidine. We also introduced *HIS3*, *HIS3-[SAE3]* and *HIS3-[PCH2]* reporter cassettes into isogenic *mud2Δ* p360-MUD2(*URA3 CEN MUD2*) and *mud1Δ* p360-MUD1(*URA3 CEN MUD1*) strains and then analyzed them as outlined above. *swt21Δ* strains harboring the reporter genes were generated through genetic manipulations involving crossing *swt21Δ::natR* cells to isogenic wild-type strains containing the *HIS3*, *HIS3-[SAE3]*, or the *HIS3-[PCH2]* reporter alleles.

RESULTS

Tgs1 methyltransferase is required for sporulation

We monitored the appearance of 4-spore asci as a function of time after transfer of a culture of yeast SK1 diploid cells to sporulation medium. Wild-type SK1 efficiently and synchronously formed asci between 8 and 12 h and attained 93% sporulation efficiency at 24 h (Figure 1A). By contrast, an isogenic *tgs1Δ* diploid was grossly defective in completion of the meiotic program, with only 4% ascus formation after 24 h (Figure 1A). Normal kinetics of sporulation were restored to the *tgs1Δ* strain by integration of a wild-type *TGS1* gene at the chromosomal *LEU2* locus (Figure 1B). The key finding was that no rescue of the sporulation defect of the *tgs1Δ* diploid was achieved by integration of the *tgs1-D126A* allele (Figure 1B). Asp126 coordinates the ribose hydroxyls of the AdoMet methyl donor in the Tgs1 active site (35). The Asp126 equivalent is essential for guanine–N2 methyltransferase activity *in vivo* and *in vitro* in all Tgs enzymes that have been studied (2,4–6). We conclude that the catalytic activity of Tgs1, and thus the TMG cap structure, is critical for the yeast meiotic developmental program.

Meiotic splicing in *tgs1Δ* cells

RNA was isolated from wild-type and *tgs1Δ* diploids immediately prior to (time 0) and 4 h and 8 h after transfer from pre-sporulation medium to sporulation medium. cDNA was prepared from each RNA sample by reverse transcription and then used for gene-specific PCR amplification of meiotic spliced transcripts (Figure 2 and Table 1). The sense and antisense primers corresponded to sequences flanking the introns so that the longer

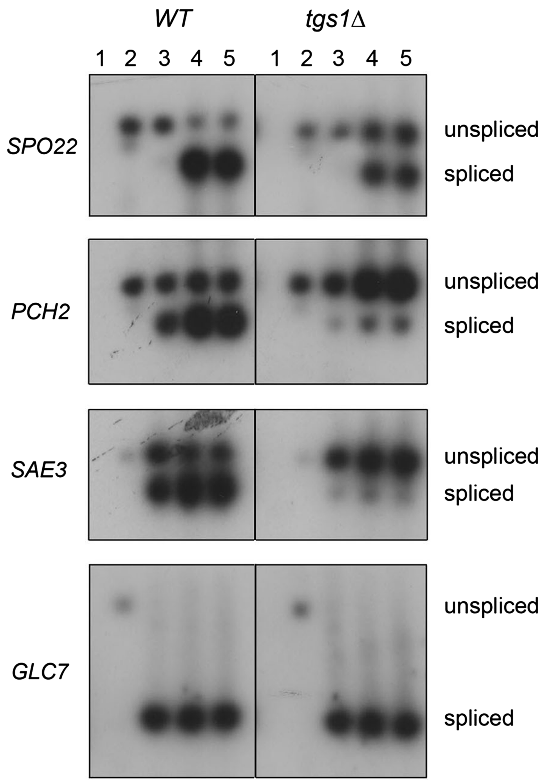

Figure 2. Meiotic splicing in *tgs1*Δ cells. RNAs isolated from wild-type and *tgs1Δ* diploid strains sampled immediately prior to transfer to sporulation medium (lane 3) or 4 h (lane 4) and 8 h (lane 5) post-transfer to sporulation medium were reverse transcribed and the cDNAs were PCR-amplified with gene-specific primers flanking the introns of meiotic transcripts *SPO22, PCH2* and *SAE3* and the constitutively spliced *GLC7* transcript. The antisense PCR primers were 5′ ^{32}P-labeled in each case. The labeled PCR products were resolved by native agarose gel electrophoresis. The RNA samples in lanes 1 were PCR-amplified without reverse transcription, as a control for potential genomic DNA contamination. Lane 2 includes aliquots of the products of PCR-amplification of genomic DNA, which are the same size as the RT–PCR products derived from the intron-containing RNAs. The RT–PCR products from wild-type (16) and *tgs1*Δ diploids were analyzed on the same gel and visualized by autoradiography. The positions of the RT–PCR products of unspliced and spliced transcripts are indicated at 'right'.

Table 1. Meiotic mRNA splicing efficiency: effects of *tgs1Δ*

RNA	*TGS1*	*tgs1Δ*
	(% spliced)	(% spliced)
AMA1	84 ± 5	32 ± 6
MER2	76 ± 2	53 ± 7
MER3	80 ± 2	29 ± 2
HOP2	88 ± 6	77 ± 2
REC114	87 ± 1	63 ± 1
MEI4	80 ± 1	39 ± 2
REC102	84 ± 4	63 ± 3
DMC1	95 ± 1	89 ± 2
PCH2	73 ± 2	8 ± 2
SAE3	66 ± 1	14 ± 1
SPO1	84 ± 3	51 ± 4
SPO22	86 ± 1	52 ± 2
MND1	90 ± 4	58 ± 3
SRC1	94 ± 2	83 ± 2

products of amplification of cDNA derived from unspliced pre-mRNAs could be easily resolved by native gel electrophoresis from the shorter products of amplification of cDNAs copied from spliced mRNA (Figure 2). One of the primers was 5′ ^{32}P-labeled in each PCR reaction so that we could quantify the distributions of unspliced and spliced cDNAs for each gene of interest (Figure 2, lanes 3–5). An aliquot of a PCR amplification reaction using genomic DNA as template provided a marker for the unspliced species (lane 2). No labeled products were generated from PCR reactions programmed by RNA that had not been subjected to prior treatment with reverse transcriptase (lane 1), indicating that the RNA samples were effectively free of contaminating genomic DNA.

Figure 2 shows exemplary data demonstrating induction of meiotic transcription and regulated meiotic splicing in wild-type cells (16), while focusing on some of the meiotic transcripts for which splicing efficiency was most acutely affected by the absence of Tgs1. Transcriptional induction of the *SPO22* gene in wild-type cells was evinced by the increase in total RT–PCR products at 4 and 8 h post-sporulation (lanes 4 and 5) compared to the level at time 0 (lane 3), which was accompanied by a sharp increase in the percentage of the RT–PCR product derived from spliced versus unspliced *SPO22* RNA. In agreement with previous studies (36,37), we also observed transcriptional induction of *PCH2* (Figure 2) and of several other intron-containing meiotic genes analyzed (data not shown). The induction of *SPO22*, *PCH2* and other meiotic genes was also evident in *tgs1*Δ cells after 4 and 8 h in sporulation medium (Figure 2 and data not shown). This result signifies that the gross defect in yeast sporulation in the absence of Tgs1 and TMG caps is not caused by an early failure in the meiotic transcriptional program. The salient finding was that the *tgs1*Δ mutation sharply inhibited the splicing of *SAE3* and *PCH2* pre-mRNAs, while having only a modest effect on splicing of the Nam8/Mer1 target *SPO22* (Figure 2). By contrast, the control *GLC7* RNA was constitutively expressed and very efficiently spliced in wild-type and *tgs1*Δ cells (Figure 2).

The results of our survey of splicing of 14 meiotic transcripts at 4 h post-induction of sporulation are compiled in Table 1, wherein each datum for splicing efficiency—[spliced/(spliced + unspliced)] × 100—is the average of three independent sporulation experiments and RT–PCR analyses. We operationally defined a severe mutational effect on meiotic splicing as one that elicits a ≥4-fold reduction in splicing efficiency compared to wild-type controls and a modest mutational effect as one that reduces efficiency by 2-fold (16). *SAE3* and *PCH2* were the only two transcripts that met our criterion for a severe meiotic splicing defect in the *tgs1*Δ strain. Ablation of Tgs1 reduced *SAE3* and *PCH2* splicing efficiencies by 9-fold and 5-fold, respectively (Table 1).

Differential requirements for Mer1 and Tgs1 in splicing of meiotic mRNAs

Regulated splicing of Mer1-dependent meiotic mRNAs can be recapitulated in vegetative yeast cells by forced expression of the Mer1 splicing enhancer protein (16,20,22,23). For example, *MER2* pre-mRNA is constitutively transcribed in vegetative cells, but is spliced inefficiently (20%) because Mer1 is absent (Figure 3A) (16). Expression of Mer1 during vegetative growth (by transformation with a 2 μ *MER1* plasmid in which *MER1* is linked to a constitutive promoter) increased *MER2* splicing efficiency to 87% in wild-type cells (Figure 3A). Mer1 expression increased *MER2* splicing efficiency in *tgs1*Δ cells from 9% to 72% (Figure 3A). To gauge the effects of Tgs1 ablation of splicing of another Mer1 target, *SPO22*, we cotransformed vegetative cells with a 2 μ plasmid bearing *SPO22* plus either a 2 μ *MER1* plasmid (Mer1+) or an empty vector control (Mer1–). Splicing of *SPO22* mRNA in wild-type yeast was acutely dependent on Mer1 (86% in Mer1-expressing cells versus 14% in control cells) (16), but not Tgs1 (56% splicing in Mer1-expressing *tgs1*Δ cells versus 3% in *tgs1*Δ control cells) (Figure 3B). We conclude that whereas loss of Tgs1 diminished basal splicing of *MER3* and *SPO22* RNAs, it did not compromise the activation of *MER3* and *SPO22*

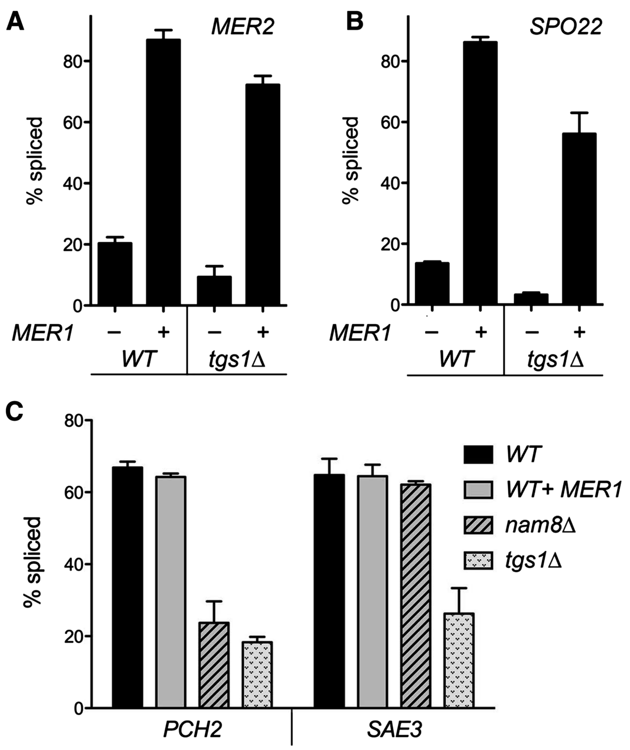

Figure 3. Requirements for meiotic splicing can be gauged in vegetative cells. Endogenous *MER2* transcripts (**A**) and transcripts derived from plasmid-borne meiotic genes *SPO22* (**B**), *PCH2* and *SAE3* (**C**) were analyzed by RT–PCR with gene-specific primers using total RNA template isolated from wild-type, *tgs1*Δ or *nam8*Δ haploids that carried either a 2 μ plasmid for constitutive expression of Mer1 (*MER1+*) or an empty 2 μ plasmid control (*MER1–*). The antisense PCR primers were 5′ ^{32}P-labeled in each case. The PCR products were analyzed by 5% native PAGE and visualized by scanning the dried gels with a phosphorimager. The RT–PCR products derived from unspliced and spliced transcripts were quantified and the splicing efficiencies (% spliced = spliced/(spliced + unspliced) × 100) are plotted. Each datum is the average of three separate experiments ± SEM.

splicing by Mer1. Previous studies showed that Mer1-activated splicing of *MER2* and *SPO22* was strictly co-dependent on Nam8 (16).

By contrast, the splicing of *PCH2* and *SAE3* transcripts, which we identified here as Tgs1-dependent, was unaffected by Mer1 expression (Figure 3C). This makes sense, given that neither of the Tgs1-dependent meiotic pre-mRNAs has a Mer1 enhancer element in the intron. The efficiencies of *PCH2* and *SAE3* splicing in wild-type vegetative cells (67% and 65%, respectively) were comparable to those seen in meiotic cells (Table 1) (16). Whereas *PCH2* splicing was reduced to similar degrees in either *nam8*Δ cells (24%) or *tgs1*Δ cells (18%), *SAE3* splicing was inhibited selectively in *tgs1*Δ cells (26% efficiency) (Figure 3C). These results consolidate the following points: (i) both examples of Tgs1-dependent splicing are independent of Mer1 and can be modeled in vegetative cells and (ii) Tgs1-dependent *SAE3* and *PCH2* pre-mRNAs differ in their codependence on Nam8.

Features of Tgs1-dependent pre-mRNAs

The Mer1/Nam8-dependent meiotic pre-mRNAs share the property that their 5′ splice sites deviate from the consensus 5′-GUAUGU motif that promotes base-pairing with the U1 snRNA during the first step of spliceosome assembly. By contrast, the Tgs1-dependent *SAE3* and *PCH2* pre-mRNAs adhere perfectly to the consensus 5′ splice site sequence. However, the *SAE3* and *PCH2* transcripts have introns that deviate from the consensus yeast branchpoint motif 5′-UACUAAC. The branchpoint is 5′-UAUUAAC in *SAE3* and 5′-CACUAAC in *PCH2*; these variants are extremely rare among yeast intron-containing genes (38). *SAE3* is further distinguished by a rare 3′ splice site element, AAG-3′, that deviates from the canonical 3′ splice site YAG-3′.

To query whether these deviant features of the *SAE3* intron confer Tgs1 dependence, we introduced mutations that restored the consensus branchpoint and 3′ splice site elements and then assayed splicing efficiency in vegetative cells by RT–PCR. Installing a perfect UAG 3′ splice site (in mutant *SAE3-3′SS*) had no salutary effect on splicing efficiency in wild-type (66%) or *tgs1*Δ (21%) cells (Figure 4). By contrast, the consensus branchpoint (entailing a U-to-C mutation in *SAE3-BP*) enhanced splicing in wild-type cells to 88%. Whereas the corrected branchpoint also raised splicing efficiency slightly in *tgs1*Δ cells (to 47%), it did not efface the dependence of *SAE3* splicing on Tgs1. Simultaneous correction of the branchpoint and 3′ splice sites in mutant *SAE3-(BP+3′SS)* provided no advantage over the single mutation of the branchpoint (Figure 4). We conclude that the non-consensus branchpoint affects *SAE3* splicing efficiency but is not the sole decisive factor in *SAE3*'s dependence on TMG caps.

Influence of RNA secondary structure in the *SAE3* intron

There is an emerging wealth of evidence attesting to the role of RNA secondary structures in regulating the splicing of specific pre-mRNAs (39). Interrogation of the potential secondary structure of the 86-nt *SAE3*

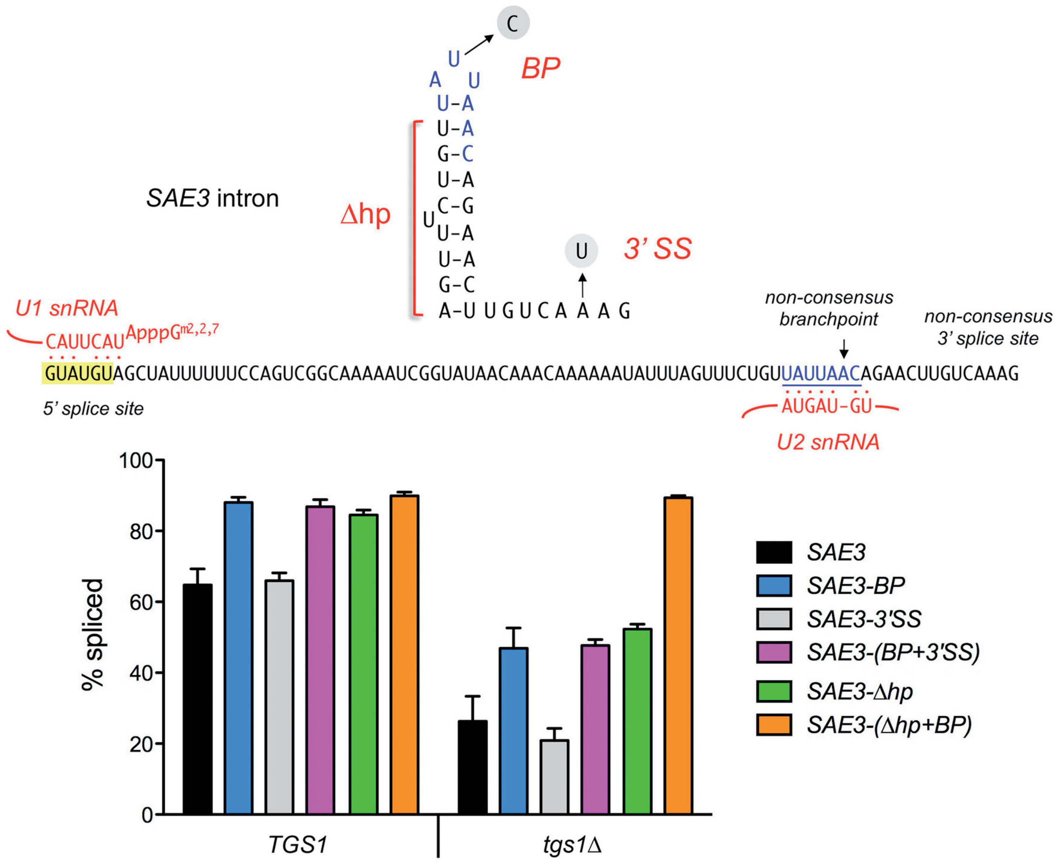

Figure 4. Intronic determinants of the Tgs1 dependence of *SAE3* pre-mRNA splicing. The nucleotide sequence of the *SAE3* intron is shown in the 'middle', highlighting its base-pairing interactions with U1 snRNA at the 5′ splice site and with U2 snRNA at the branchpoint. An Mfold-predicted hairpin (hp) structure is shown encompassing the branchpoint (upper panel). The local deletion mutation (*Δhp*) and point mutations (*BP* and *3′SS*) that we introduced into the *SAE3* intron are indicated. Splicing was gauged by RT–PCR with *SAE3*-specific primers using total RNA template isolated from wild-type or *tgs1Δ* haploids that had been transformed with 2 μ *SAE3* or its intron mutant variants as specified. The antisense PCR primer was 5′ ^{32}P-labeled. The RT–PCR products derived from unspliced and spliced transcripts were resolved by native 5% PAGE and quantified. The splicing efficiencies are plotted as sets for the *TGS1* and *tgs1Δ* strains (bottom left). Each datum is the average of three separate experiments ± SEM.

intron in Mfold (40) revealed a single predicted fold (Δ*G* -11.7) containing a stem–loop structure of immediate interest with respect to regulatory potential (Figure 4). This stem–loop, from nucleotides 57 to 78, consists of a 9-bp stem with one bulged base plus an apical triloop. This predicted structure embraces the 5′-UAUUAAC branchpoint element within the apical stem and loop, in a manner that would mask the intermolecular base-pairing interactions of the branchpoint sequence to U2 snRNA (Figure 4) that are critical for the next step of spliceosome assembly. Thus, this intronic secondary structure might pose a barrier to efficient *SAE3* pre-mRNA splicing that is overcome by Tgs1 and TMG caps.

To evaluate this scenario, we made a short internal deletion in the *SAE3* intron—of nucleotides 57–65 (Δ*hp*)—that is predicted to abolish the RNA hairpin structure (Figure 4). An instructive finding was that disruption of the stem–loop covering the branchpoint by the Δ*hp* mutation increased splicing efficiency in both wild-type and *tgs1Δ* cells, to 84% and 53%, respectively, but still did not efface the contribution of Tgs1 to *SAE3* splicing. The decisive maneuver was to introduce the Δ*hp* deletion into the *SAE3-BP* intron, which resulted in equivalently high (90%) splicing efficiencies in wild-type and *tgs1Δ* cells (Figure 4). We conclude that the reliance of *SAE3* splicing on Tgs1 and TMG caps reflects the doubly unfavorable primary and secondary structure of the branchpoint in the *SAE3* intron.

The *SAE3* intron is a portable determinant of Tgs1 dependence

We inserted the 86-nt *SAE3* intron near the 5′ end of the otherwise intron-less chromosomal yeast *HIS3* gene in both *TGS1* and *tgs1Δ* haploid yeast cells (Figure 5A). *HIS3* provides a convenient reporter for gene expression, manifest as histidine prototrophy (*HIS3* 'on') or auxotrophy (*HIS3* 'off'). The native *HIS3* gene is functional in *TGS1* and *tgs1Δ* strains, both of which grow on agar medium lacking histidine (Figure 5B). By contrast, the *HIS3-[SAE3]* reporter containing the inserted *SAE3* intron was functional in *TGS1* cells, but not in the *tgs1Δ* background (Figure 5B). The salient finding was that the Δ*hp* mutation disrupting the stem–loop covering

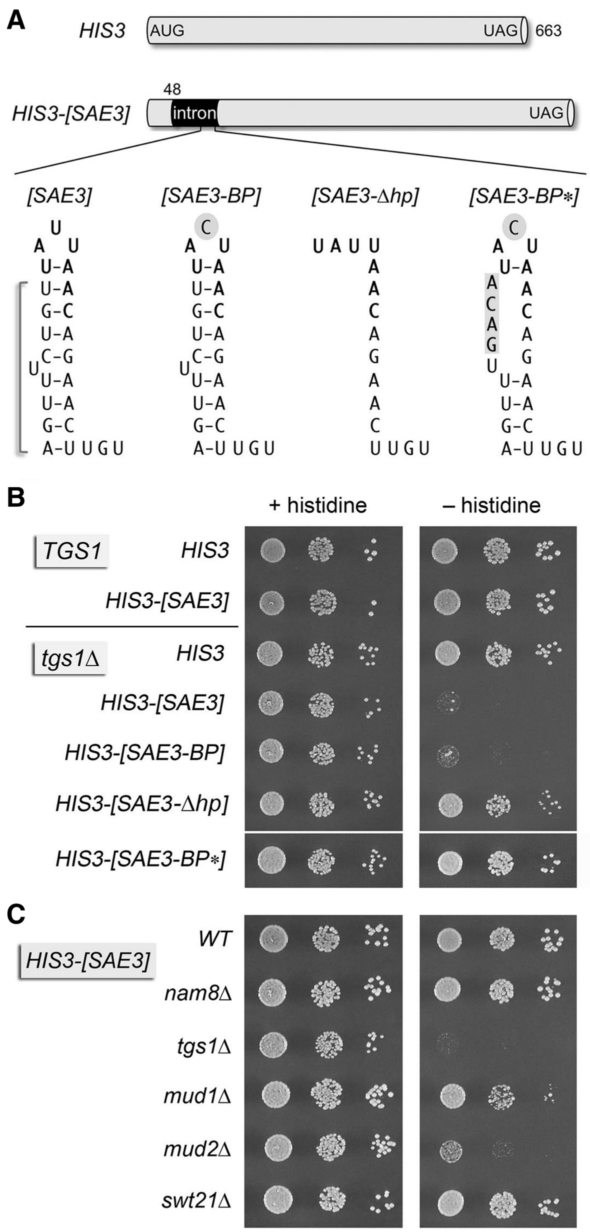

Figure 5. The *SAE3* intron is a portable determinant of Tgs1 dependence. (**A**) Schematic depiction of the *HIS3* reporter genes. The *HIS3* ORF is shown in gray; the *SAE3* intron is colored black. The branchpoint sequences and predicted secondary structures are shown in the expanded view. (**B**) Serial dilutions of isogenic *TGS1* and *tgs1*Δ cells harboring the indicated chromosomal *HIS3* cassettes were spotted in parallel on synthetic dropout medium containing or lacking histidine as specified. The plates were photographed after incubation for 2 days at 30°C. (**C**) The indicated strains harboring a chromosomal *HIS3-[SAE3]* reporter were analyzed as described for panel B.

the branchpoint restored *HIS3* function in *tgs1*Δ cells (Figure 5B). By contrast, the U-to-C mutation in *SAE3-BP* that restored a consensus branchpoint sequence did not suffice *per se* to confer histidine prototrophy in *tgs1*Δ cells. However, combining the consensus branchpoint U-to-C mutation with an upstream 4-nt substitution that prevents base pairing of this segment to the branchpoint restored *HIS3* function in *tgs1Δ* cells (Figure 5B). These results show that the *SAE3* intron, by virtue of its branchpoint context, is an autonomous determinant of Tgs1-dependence in the absence of other *SAE3* gene elements (i.e. promoter, 5′ and 3′ exons, 5′ and 3′ untranslated regions). Thus, TMG caps are implicated in recognition and/or utilization of the deviant *SAE3* branchpoint.

The specificity of the splicing factor requirements for *HIS3-[SAE3]* reporter function was tested by introducing the expression cassette into the chromosome of yeast strains deleted for four other vegetatively inessential splicing factors—Nam8, Mud1, Mud2, and Swt21—that display synthetic lethal/sick interactions with one another and with Tgs1 (6,8,16). We found that *HIS3-[SAE3]* was active in *nam8*Δ, *mud1*Δ and *swt21*Δ cells, but not in *mud2*Δ cells (Figure 5C). The finding that Mud2 facilitates expression of a pre-mRNA with a suboptimal branchpoint region is consistent with Mud2 being a component of a heterodimeric complex with the yeast branchpoint binding protein Msl5 (41).

SAE3 pre-mRNA splicing *in vitro*

We extended our analysis of intronic determinants of *SAE3* splicing by testing the wild-type and mutated *SAE3* RNAs as substrates for splicing *in vitro* in a whole-cell extract prepared from a *TGS1* yeast strain. The *SAE3* DNA constructs were cloned downstream of a bacteriophage RNA polymerase promoter and *SAE3* pre-mRNAs with 5′ m^7G caps and internal ^{32}P-GMP-labels were prepared by cap dinucleotide-primed transcription *in vitro* by phage RNA polymerase (Supplementary Figure S1). The isolated pre-mRNAs were incubated with yeast whole-cell extract under optimized splicing conditions (42) and the radiolabeled products were resolved by polyacrylamide gel electrophoresis (PAGE) and visualized by autoradiography. Splicing was manifest as the conversion of the unspliced precursor into a shorter mature spliced product (Figure 6). Splicing efficiency was quantified by the distribution of radiolabel [spliced/(spliced + unspliced)] after correction for the ^{32}P-GMP content of the two species. The salient finding was that *in vitro* splicing of the wild-type *SAE3* intron was conspicuously inefficient (7%), but was responsive to manipulations of the intron in a manner concordant with the *in vivo* data presented above. To wit, splicing was enhanced by installation of a consensus branchpoint (36%) and disruption of the predicted branchpoint secondary structure (38%), whereas there was no salutary effect of restoring a consensus 3′ splice site (9%) (Figure 6). Combining the consensus branchpoint with the relief of secondary structure over the branchpoint exerted additive effects that resulted in 89% *SAE3* splicing efficiency *in vitro* (Figure 6), a value comparable to the 83% efficiency of splicing of actin pre-mRNA in the same experiment (data not shown).

Having established that several of the *SAE3* pre-mRNAs can be spliced *in vitro*, we compared their efficacies in whole-cell extracts derived from otherwise isogenic *TGS1* and *tgs1*Δ yeast strains. The kinetic profiles of actin pre-mRNA splicing were similar in the two extracts (Figure 7A), as were the rates and extents of splicing of the intron-containing U3 pre-snoRNA (data not shown). These results signify that TMG cap structures on the endogenous spliceosomal snRNAs are not limiting for removing the introns of pre-RNAs that are normally spliced with high efficiency *in vitro*. By contrast, the rates and extents of splicing of the *SAE3-BP* and *SAE3-Δhp* pre-mRNAs in the *TGS1* extract were lower than that of actin pre-mRNA; moreover, the *SAE3-BP* and *SAE3-Δhp* substrates experienced a kinetic delay in the initial appearance of their respective mature spliced products (Figure 7B and C). A key finding was that the rate and extent of *SAE3-BP* splicing was ∼3-fold lower in *tgs1Δ* extracts than in *TGS1* extracts (Figure 7B). The *SAE3-Δhp* substrate was spliced nearly 2-fold slower in *tgs1Δ* extracts than in *TGS1* extracts (Figure 7C). The disparity in *SAE3* versus actin pre-mRNA splicing in the *TGS1* extract was erased by the *SAE3-(Δhp+BP)* intron (Figure 7D), which also corrected the lag in splicing onset seen with the *SAE3-BP* and *SAE3-Δhp* substrates. The *SAE3-(Δhp+BP)* intron also expunged the disparity in *SAE3* splicing rates in *TGS1* versus *tgs1Δ* extracts (Figure 7D). Thus, the requirements for bypassing TMG cap-dependence of *SAE3* splicing *in vivo* were recapitulated *in vitro*.

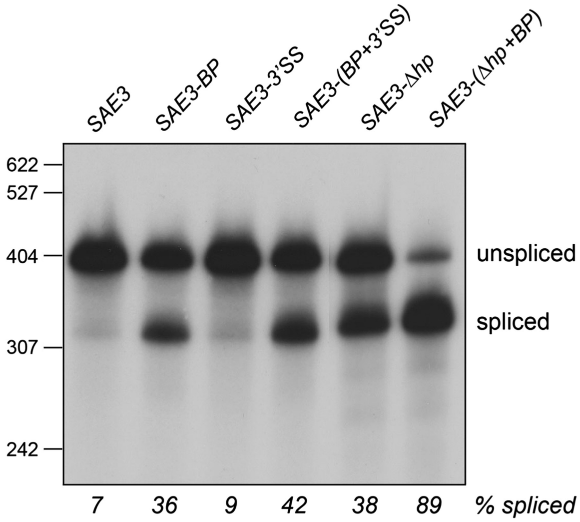

Figure 6. *SAE3* pre-mRNA splicing *in vitro*. ^{32}P-GMP-labeled *SAE3* pre-mRNAs as specified were incubated in whole-cell *TGS1* extracts for 20 min at 28°C. The splicing reaction products were analyzed by denaturing PAGE and autoradiography. The splicing efficiencies are shown at the bottom of each lane. The positions and sizes (nt) of ^{32}P-labeled denatured DNA markers (Msp1 fragments of pBR322) are indicated on the 'left'.

Determinants of the Tgs1 dependence of *PCH2* splicing

The *PCH2* transcript is distinguished by its exceptionally long 5′ exonic open reading frame (1551-nt) and a non-consensus intron branchpoint sequence, 5′-CACUA AC (Figure 8). We probed the *PCH2* splicing determinants by: (i) installing a consensus branchpoint sequence in an otherwise native *PCH2* gene; (ii) deleting most of the long upstream exon (while installing a new in-frame AUG codon) to create a *PCH2-Δ5′* variant with a 51-nt 5′ exon; and (iii) combining the *BP* and *Δ5′exon* changes. We tested the *PCH2* mutants on 2 μ plasmids for their splicing efficiency in *TGS1* and *tgs1Δ* yeast cells. As noted previously (16), the results implicate the non-consensus branchpoint and long 5′ exon as separate

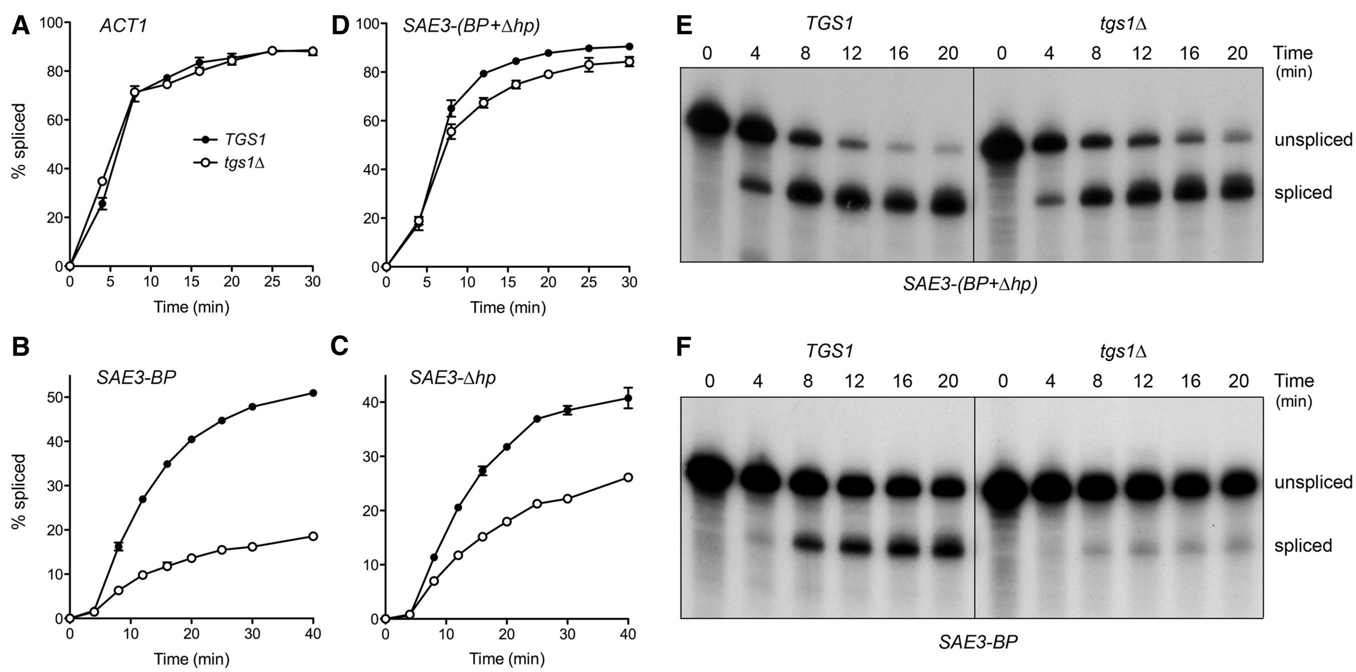

Figure 7. TMG dependence of *SAE3* pre-mRNA splicing *in vitro* is dictated by the branchpoint. The kinetics of splicing of ^{32}P-GMP-labeled *ACT1* (**A**), *SAE3-BP*, (**B**), *SAE3-Δhp* (**C**), and *SAE3-(BP+Δhp)* (**D**) pre-mRNAs in *TGS1* (filled circle) and *tgs1Δ* (open circle) extracts are shown. Each datum is the average of three independent experiments ±SEM. Representative analyses of the products of splicing of the *SAE3-(BP+Δhp)* pre-mRNA (**E**) and the *SAE3-BP* pre-mRNA (**F**) by denaturing PAGE and autoradiography are shown.

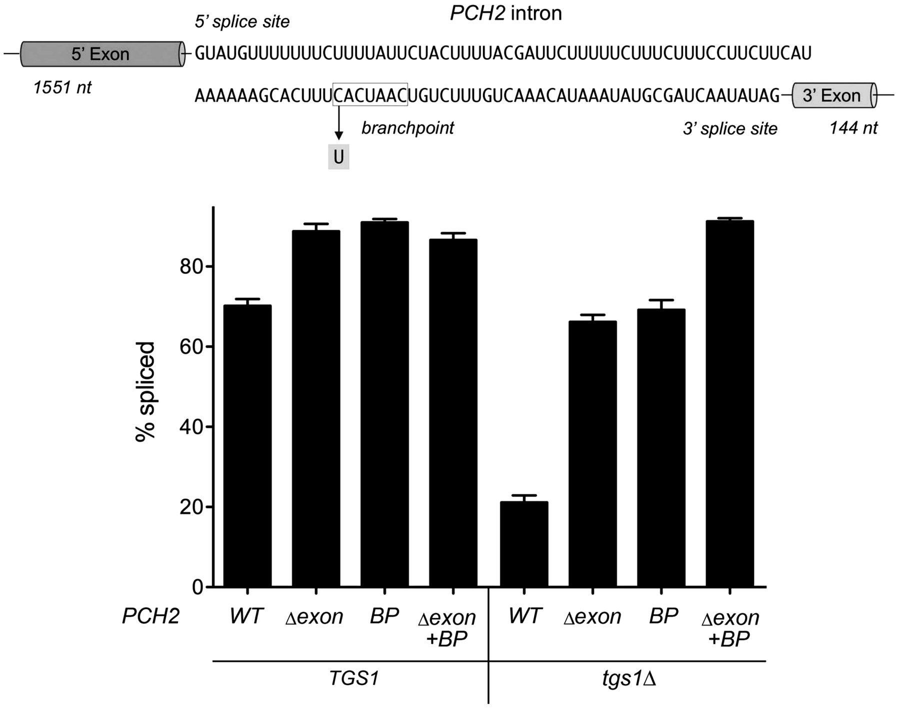

Figure 8. Determinants of the Tgs1 dependence of *PCH2* pre-mRNA splicing. The nucleotide sequence of the *PCH2* intron is shown, highlighting its non-consensus branchpoint and the intronic C-to-U mutation (*BP*) mutation that restored a consensus element. The sizes of the flanking protein encoding 5′ and 3′ exons are indicated. The 5′ coding exon in the Δ*exon* mutant was shortened to 51 nt. Splicing was gauged by RT–PCR with *PCH2*-specific primers using total RNA template isolated from wild-type (*TGS1*) (16) or *tgs1*Δ haploids that had been transformed with 2 μ *PCH2* or its *BP* or Δ*exon* mutant variants as specified. The splicing efficiencies are plotted. Each datum is the average of six separate experiments ± SEM.

negative influences on *PCH2* splicing in wild-type cells. For example, shortening the 5′ exon *per se* increased splicing efficiency to 89% for *PCH2-Δexon* versus 70% for the *PCH2* transcript (Figure 8). The consensus branchpoint change *per se* increased splicing efficiency to 91% for *PCH2-BP* (Figure 8). There was no apparent effect of combining the *BP* and *Δexon* changes in wild-type cells. The *PCH2* transcript was spliced with 21% efficiency in *tgs1Δ* cells, a 3.5-fold decrement compared to *TGS1* cells. The *PCH2-Δexon* transcript was spliced at 66% efficiency in *tgs1*Δ cells, signifying that shortening the 5′ exon overrode much of the Tgs1 requirement (Figure 8). The *PCH2-BP* transcript was spliced with 69% efficiency in *tgs1Δ* cells, implying that the non-consensus branchpoint is an independent determinant of Tgs1-dependence of *PCH2* splicing. Combining the BP and exon changes elicited a further gain of splicing in *tgs1Δ* cells to 91% (Figure 8), the same as the maximum level attained in wild-type cells. Thus, the TMG requirement for *PCH2* splicing is governed by two features of the pre-mRNA: the intron and its deviant branchpoint sequence and the long 5′ exon.

The *PCH2* intron and 5′ exon length are portable determinants of Tgs1 dependence

We inserted the 113-nt *PCH2* intron within the chromosomal yeast *HIS3* gene of *TGS1* and *tgs1*Δ haploid yeast cells (Figure 9A). The *PCH2* intron was placed near the 3′ end of the *HIS3* ORF to reflect its distal position in the native *PCH2* pre-mRNA. The *HIS3-[PCH2]* gene containing the inserted *PCH2* intron was functional in *TGS1* cells (as gauged by growth on agar medium lacking histidine) but not in the *tgs1Δ* background (Figure 9B). The instructive finding here was that a single C-to-U mutation in the intron of the *HIS3-[PCH2]* reporter that restored a consensus branchpoint (Figure 9A) sufficed to restore *HIS3* function in *tgs1*Δ cells (Figure 7B). These results show that the *PCH2* intron, by virtue of its deviant branchpoint, is an autonomous determinant of Tgs1-dependence in the absence of other *PCH2* gene elements. To evaluate the contributions of 5′ exon length to the Tgs1-dependence of *PCH2* intron removal, we repositioned the intron proximally within the *HIS3* reporter (inserting it at the same site used to generate the *HIS3-[SAE3]* reporter). This maneuver sufficed to allow *tgs1*Δ cells to grow in the absence of added histidine (Figure 9B). These results implicate TMG caps in recognition and/or utilization of the non-consensus *PCH2* branchpoint in the context of a pre-mRNA substrate with a relatively long 5′ exon.

The specificity of the splicing factor requirements for *HIS3-[PCH2]* reporter function was tested by introducing the expression cassette into the chromosome of yeast strains deleted for other vegetatively inessential splicing factors that display synthetic lethal/sick interactions with one another and with Tgs1. As expected, expression of the *HIS3-[PCH2]* reporter was impaired in *nam8*Δ cells (Figure 9C), consistent with the Nam8

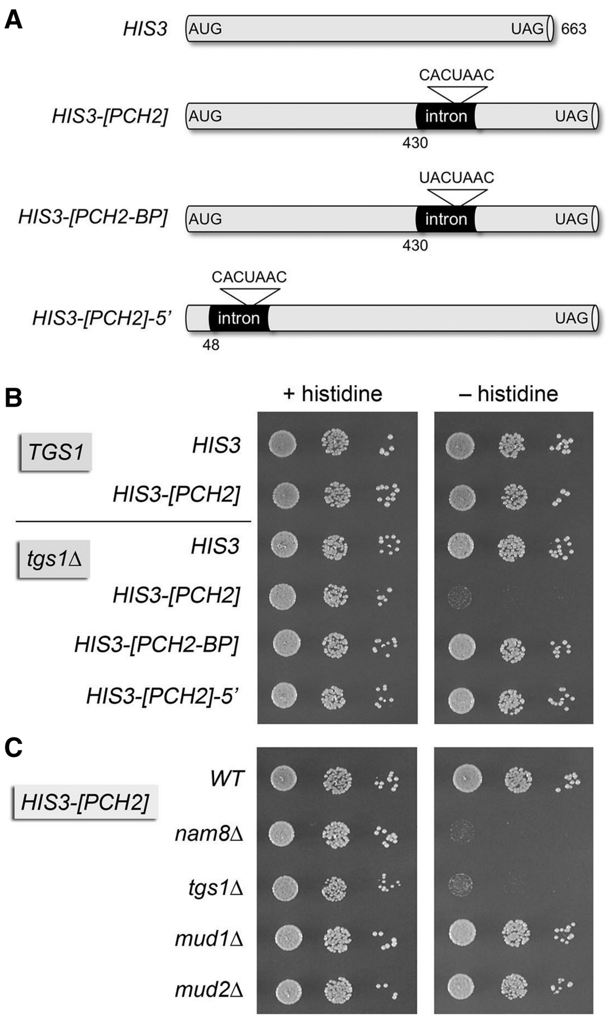

Figure 9. The *PCH2* intron and 5′ exon length are portable determinants of Tgs1 dependence. (**A**) Schematic depiction of the *HIS3* reporter genes. The *HIS3* ORF is shown in gray; the *PCH2* introns are colored black with the branchpoint sequence in the expanded view. (**B**) Serial dilutions of isogenic *TGS1* and *tgs1*Δ cells harboring the indicated chromosomal *HIS3* cassettes were spotted in parallel on synthetic dropout medium containing or lacking histidine as specified. The plates were photographed after incubation for 2 days at 30°C. (**C**) The indicated strains harboring a chromosomal *HIS3-[PCH2]* reporter were analyzed as described for panel B.

requirement for *PCH2* pre-mRNA splicing during meiosis (16). The instructive findings were that *HIS3-[PCH2]* was active in *mud1*Δ and *mud2*Δ cells (Figure 9C) and in *swt21*Δ cells (data not shown).

DISCUSSION

The inessentiality of Tgs1 and TMG caps for vegetative growth of budding and fission yeast (2,5) is paradoxical in light of the presence of TMG caps on the essential spliceosomal U1, U2, U4 and U5 snRNAs of nearly all eukaryal taxa (43). Synthetic genetic array analysis in budding yeast revealed that the effects of ablating the TMG cap are buffered by spliceosome assembly factors, that are themselves inessential for vegetative growth (6,11). Thus, Nature has overlaid genetic redundancy on an ancient eukaryal-specific RNA modification (the TMG cap) that participates in a defining step of eukaryal RNA biogenesis (spliceosome-catalyzed intron removal). This raises the important question of what RNA transactions, if any, are TMG cap-dependent *per se*.

The present finding that the absence of TMG caps on all yeast snRNAs does not impact *in vitro* splicing of intron-containing actin and U3 pre-RNAs is a biochemical validation of the genetic data that TMG caps are dispensable for yeast cell growth and, perforce, for adequate levels of *in vivo* splicing of the many intron-containing RNAs needed for vegetative growth under laboratory conditions. Earlier depletion–reconstitution studies with mammalian cell extracts had shown that that individual human U1, U2, U4 and U5 snRNPs could be reconstituted singly in a splicing-competent state from the respective synthetic snRNAs lacking a TMG cap structure (44–47). However, in U2 snRNA-depleted frog oocytes, a TMG cap was required for reconstitution of splicing by injected synthetic U2 snRNA (48). These seemingly contradictory findings regarding U2 function hinted that reliance on TMG caps for splicing might vary with cell type or developmental stage. The idea of context-dependent TMG requirements gained traction with the report that Tgs1 methyltransferase activity is critical during a discrete temporal phase of *Drosophila* early pupal development (10).

Here, we show that Tgs1 and TMG caps are essential for execution of the meiotic developmental program in budding yeast. We correlate the failure of *tgs1*Δ diploids to sporulate with a specific deficit in splicing of two meiotic pre-mRNAs—*SAE3* and *PCH2*. *SAE3* had not been recognized previously as a genetically vulnerable target of splicing control. *PCH2* was identified recently as a novel target for Mer1-independent Nam8-dependent meiotic splicing control (16). Sae3 is essential for meiosis and sporulation (49), whereas Pch2, a meiotic checkpoint protein, is not normally required for sporulation in an otherwise wild-type background (50). Although it is conceivable that the severe defect in *SAE3* splicing might explain the sporulation deficiency of the *tgs1*Δ strain, the modest decrements in splicing of *AMA1* and *MER3* pre-mRNAs in *tgs1*Δ cells (2.5-fold at 4 h; Table 1) could also contribute to the phenotype. Note that *AMA1* and *MER3* each have one of the characteristics of Tgs1-dependent meiotic pre-mRNA targets, to wit: (i) *AMA1*, like *PCH2*, has an exceptionally long 5′ exon (1183-nt); and (ii) *MER3* has a deviant branchpoint sequence (5′-GACUAAC).

Tgs1-dependent meiotic splicing is novel *vis-à-vis* the Mer1-driven mechanism characterized previously (23). Mer1 upregulates splicing of four meiotic transcripts: *AMA1*, *MER2*, *MER3* and *SPO22*. All Mer1-regulated meiotic transcripts share three properties: (i) they have non-consensus 5′ splice sites; (ii) they have an intronic enhancer sequence to which Mer1 binds and (ii) they are co-dependent for splicing on Nam8 (Figure 10). By contrast, the Tgs1-dependent *SAE3* and *PCH2* transcripts have consensus 5′ splice sites and lack Mer1 intronic enhancer elements. The two Tgs1-dependent transcripts

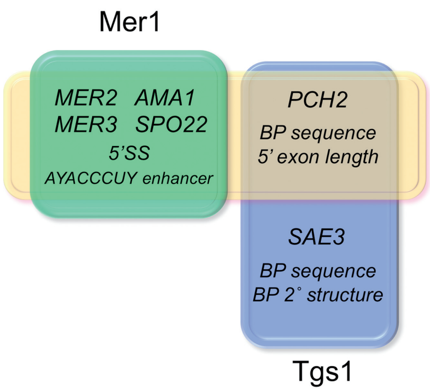

Figure 10. Three genetically distinct meiotic splicing regulons. The Venn-like diagram illustrates the meiotic pre-mRNAs that comprise the Mer1/Nam8-codependent, Nam8/Tgs1-codependent, and Tgs1-dependent splicing regulons. The pre-mRNA features that govern each regulon are listed below the target genes.

diverge with respect to whether they do (*PCH2*) or do not (*SAE3*) co-depend on Nam8 for their splicing during meiosis (Figure 10). The Tgs1-dependent transcripts also differ as to whether excision of their introns does (*SAE3*) or does not (*PCH2*) co-depend on Mud2 (Figures 5 and 9).

The positive impact of TMG caps on *SAE3* and *PCH2* pre-mRNA splicing is evinced in vegetative yeast cells, by comparing splicing efficiency in *TGS1* versus *tgs1*Δ haploids. We infer that there are probably no strictly meiosis-specific positive coregulators of TMG dependency. Indeed, we see that vegetative splicing of *SAE3* and *PCH2* is unaffected by forced expression of Mer1, the only known meiosis-specific splicing regulator (26). The residual levels of *SAE3* and *PCH2* splicing in *tgs1*Δ haploids (26% and 18%, respectively) are somewhat higher than the corresponding splicing levels in *tgs1*Δ diploids undergoing meiosis (14% and 8%, respectively). Nonetheless, the reliable differences in splicing efficiencies of Tgs1-dependent transcripts in vegetative cells allowed for analysis of the RNA determinants of meiotic splicing in vegetative cells that do or do not have TMG caps.

Here, we focused predominantly on *SAE3*, the meiotic transcript that depends uniquely on Tgs1 (but not Nam8) for efficient splicing *in vivo*. The *SAE3* intron has non-consensus branchpoint and 3′ splice site signals, either of which could conceivably enfeeble *SAE3* splicing and make it more sensitive to factors that are inessential for splicing of consensus introns. It proved the case that the primary and secondary structures of the *SAE3* branchpoint are key determinants of splicing efficiency and Tgs1 dependence, whereas the 3′ splice site had no obvious impact on either parameter. We demonstrated additive negative effects of the non-consensus branchpoint sequence and the predicted hairpin fold in which the branchpoint is embedded. Simultaneously restoring a consensus UACUAAC sequence and eliminating the potential for hairpin formation enhanced the efficiency of *SAE3* splicing in *TGS1* cells and abolished the differential in *SAE3* splicing efficiency in *tgs1*Δ cells. The *SAE3* intron *per se* is a portable determinant of Tgs1-dependent gene expression when transferred to the otherwise intron-less *HIS3* gene. This result is important, because it militates against a scenario in which the requirement for TMG caps is enforced in *cis*, i.e. if the *SAE3* pre-mRNA is itself targeted for TMG capping in *TGS1* cells via some distinctive property of the *SAE3* transcription unit (*a la* TMG capping of a fraction of RRE-containing HIV-1 pre-mRNAs in human cells; (51). In the *HIS3* reporter context, the secondary structure of the *SAE3* branchpoint is the dominant factor in Tgs1 dependence, i.e. deleting the proximal stem that embeds the *SAE3* branchpoint restored histidine prototrophy to *tgs1*Δ cells. Changing the sequence of the proximal stem so as to prevent base pairing to the branchpoint (without deleting any nucleotides) also restored histidine prototrophy to *tgs1*Δ cells, when combined with U-to-C change in the branchpoint.

We recapitulated features of *SAE3* splicing control in an *in vitro* splicing system. The yeast whole-cell extract efficiently excised introns from synthetic pre-RNAs derived from yeast transcripts that are known to be spliced well *in vivo* (e.g. actin and U3). By contrast, a synthetic *SAE3* pre-mRNA was a conspicuously feeble substrate for splicing *in vitro*, as a consequence of the same negative influences at the branchpoint that affected *SAE3* splicing *in vivo*. The extent of splicing of wild-type *SAE3* intron *in vitro* (7%) was lower than the steady-state splicing level *in vivo* in vegetative cells (65%). This disparity could reflect the beneficial effects of cotranscriptional pre-mRNA processing in the yeast nucleus *in vivo* that are not attainable during splicing of an exogenous pre-mRNA in a yeast extract *in vitro*. Yet, our finding that simultaneous installation of a consensus branchpoint and elimination of the branchpoint hairpin allowed highly efficient splicing of the *SAE3-(BP+Δhp)* pre-mRNA—in *TGS1* and *tgs1*Δ extracts—validated the *in vitro* system as a gauge of *cis*-acting determinants of *SAE3* splicing.

The partial gain of *in vitro* splicing elicited by the single *SAE3-BP* and *SAE3*-Δ*hp* intron mutations allowed us to probe whether the absence of TMG caps on spliceosomal U snRNAs affected *SAE3* splicing. The findings that splicing of these *SAE3* introns was enhanced in *TGS1 versus tgs1*Δ extracts provided direct confirmation of the *in vivo* splicing phenotypes for these pre-mRNAs seen in *TGS1* and *tgs1*Δ haploid cells and verified the independent influences of branchpoint sequence and secondary structure on the TMG cap-dependency of splicing. To our knowledge, this is the first instance in which an aspect of yeast meiotic splicing control has been modeled *in vitro*.

Our presumption, based on the gain-of-function branchpoint context changes, is that the TMG requirement for *SAE3* splicing in meiosis pertains to a particular TMG-capped U snRNA (e.g. U2) or subset of snRNAs (e.g. U2 and U1) that orchestrate early spliceosome assembly and branchpoint recognition. We observed no accumulation of *SAE3* splicing intermediates (e.g. lariat intron and 5′ exon) in *TGS1* or *tgs1*Δ extracts, hinting that TMG exerts its effect during spliceosome assembly. A key question is whether TMG caps act directly to facilitate early steps in splicing (e.g. via TMG-to-RNA or TMG-to-protein interactions) or indirectly, whereby the absence of TMG caps affects snRNP structure or stability. It was reported that *tgs1*Δ yeast cells have grossly normal steady-state levels of spliceosomal snRNAs (2,5) and display no aberration in the sedimentation profiles of their spliceosomal snRNPs (2). We recently documented that affinity-purified snRNPs from *TGS1* versus *tgs1*Δ *S. cerevisiae* cells are indistinguishable with respect to overall yield, snRNA content, and the sizes of the individual snRNAs (Schwer,B., Erjument-Bromage,H. and Shuman,S., manuscript in preparation). Our analysis of the polypeptide compositions of SmB affinity-purified snRNPs showed that the snRNPs from *tgs1*Δ cells were not lacking in any of the protein components found in the snRNPs from *TGS1* cells (Schwer,B., Erjument-Bromage,H. and Shuman,S., manuscript in preparation). Such results suggest that the splicing phenotypes associated with Tgs1 deficiency are not caused by gross changes in snRNP biogenesis or structure. Further dissection of the role of the TMG cap will ultimately hinge on reconstituting *SAE3* splicing *in vitro* with combinations of individual TMG-capped and m^7G-capped snRNPs purified from *TGS1* cells and *tgs1*Δ cells, respectively.

We find that the *PCH2* pre-mRNA has different determinants of Tgs1-dependency than *SAE3*. *PCH2* has a non-consensus branchpoint sequence, 5′-CACUAAC, albeit without any predicted secondary structure when the intron is analyzed by Mfold. The *PCH2* transcript is distinguished by its exceptionally long 5′ exon. Our studies of *PCH2* splicing implicate the non-consensus branchpoint and long 5′ exon as separable negative influences on *PCH2* splicing in *TGS1* cells and as concerted determinants of the Tgs1-dependence of *PCH2* splicing (Figure 10). The separable negative effects of 5′ exon length and deviant BP sequence were also evident when the *PCH2* intron was imported to the *HIS3* gene. (Here again, we take this to mean that the Tgs1 requirement is not imposed by hypermethylation of the *PCH2* pre-mRNA.)

The elucidation of three genetically distinct meiotic splicing regulons, each with its own governing RNA determinants (Figure 10), highlights new modes of tunable RNA splicing in yeast (i.e. by TMG caps) and an unexpected richness of RNA controls during the budding yeast meiotic program.

SUPPLEMENTARY DATA

Supplementary Data are available at NAR online.

ACKNOWLEDGEMENTS

We thank Olivia Orta for expert technical assistance. S.S. is an American Cancer Society Research Professor.

FUNDING

U.S. National Institutes of Health grants GM52470 (to S.S.) and GM50288 (to B.S.). Funding for open access charges: NIH grants (GM52470 and GM50288).

Conflict of interest statement. None declared.

REFERENCES

1. Busch,H., Reddy,R., Rothblum,L. and Choi,Y.C. (1982) SnRNAs, SnRNPs, and RNA processing. *Annu Rev. Biochem.*, **51**, 617–654.
2. Mouaikel,J., Verheggen,C., Bertrand,E., Tazi,J. and Bordonné,R. (2002) Hypermethylation of the cap structure of both yeast snRNAs and snoRNAs requires a conserved methyltransferase that is localized to the nucleolus. *Mol. Cell*, **9**, 891–901.
3. Hausmann,S. and Shuman,S. (2005) Specificity and mechanism of RNA cap guanine–N2 methyltransferase (Tgs1). *J. Biol. Chem.*, **280**, 4021–4024.
4. Hausmann,S. and Shuman,S. (2005) *Giardia lamblia* RNA cap guanine-N2 methyltransferase (Tgs2). *J. Biol. Chem.*, **280**, 32101–32106.
5. Hausmann,S., Ramirez,A., Schneider,S., Schwer,B. and Shuman,S. (2007) Biochemical and genetic analysis of RNA cap guanine–N2 methyltransferases from *Giardia lamblia* and *Schizosaccharomyces pombe*. *Nucleic Acids Res.*, **35**, 1411–1420.
6. Hausmann,S., Zheng,S., Costanzo,M., Brost,R.L., Garcin,D., Boone,C., Shuman,S. and Schwer,B. (2008) Genetic and biochemical analysis of yeast and human cap trimethylguanosine synthase: functional overlap of TMG caps, snRNP components, pre-mRNA splicing factors, and RNA decay pathways. *J. Biol. Chem.*, **283**, 31706–31718.
7. Benarroch,D., Jankowska-Anyszka,M., Stepinski,J., Darzynkiewicz,E. and Shuman,S. (2010) Cap analog substrates reveal three clades of cap guanine–N2 methyltransferases with distinct methyl acceptor specificities. *RNA*, **16**, 211–220.
8. Chang,J., Schwer,B. and Shuman,S. (2010) Mutational analyses of trimethylguanosine synthase (Tgs1) and Mud2: proteins implicated in pre-mRNA splicing. *RNA*, **16**, 1018–1031.
9. Lemm,I., Girard,C., Kuhn,A.N., Watkins,N.J., Schneider,M., Bordonné,R. and Lührmann,R. (2006) Ongoing U snRNP biogenesis is required for the integrity of Cajal bodies. *Mol. Biol. Cell*, **17**, 3221–3231.
10. Komonyi,O., Papai,G., Enunlu,I., Muratoglu,S., Pankotai,T., Kopitova,D., Maróy,P., Udvarty,A. and Boros,I. (2005) DTL, the *Drosophila* homolog of PIMT/Tgs1 nuclear receptor coactivator-interacting protein/RNA methyltransferase, has an essential role in development. *J. Biol. Chem.*, **280**, 12397–12404.
11. Wilmes,G.M., Bergkessel,M., Bandyopadhyay,S., Shales,M., Braberg,H., Cagney,G., Collins,S.R., Whitworth,G.B., Kress,T.L., Weissman,J.S. *et al.* (2008) A genetic interaction map of RNA-processing factors reveals links between Sem1/Dss1-containing complexes and mRNA export and splicing. *Mol. Cell*, **32**, 735–746.
12. Gottschalk,A., Tang,J., Puig,O., Salgado,J., Neubauer,G., Colot,H.V., Mann,M., Séraphin,B., Rosbash,M., Lührmann,R. *et al.* (1998) A comprehensive biochemical and genetic analysis of the yeast U1 snRNP reveals five novel proteins. *RNA*, **4**, 374–393.
13. Puig,O., Gottschalk,A., Fabrizio,P. and Séraphin,B. (1999) Interaction of the U1 snRNP with nonconserved intronic sequences affects 5′ splice site selection. *Genes Dev.*, **13**, 569–580.
14. Del Gatto-Konczak,F., Bourgeois,C.F., Le Guiner,C., Hoster,L., Gesnel,M., Stevenin,J. and Breathnach,R. (2000) The RNA-binding protein TIA-1 is a novel mammalian splicing regulator acting through intron sequences adjacent to a 5′ splice site. *Mol. Cell. Biol.*, **20**, 6287–6299.
15. Förch,P., Puig,O., Kedersha,N., Martínez,C., Granneman,S., Séraphin,B., Anderson,P. and Valcárcel,J. (2000) The aopoptosis-promoting factor TIA-1 is a regulator of alternative pre-mRNA splicing. *Mol. Cell*, **6**, 1089–1098.
16. Qiu,Z.R., Schwer,B. and Shuman,S. (2011) Determinants of Nam8-dependent splicing of meiotic pre-mRNAs. *Nucleic Acids Res.*, January 5 (doi: 10.1093/nar/gkq1328; epub ahead of print).
17. Abovich,N., Liao,X.C. and Rosbash,M. (1994) The yeast MUD2 protein: an interaction with PRP11 defines a bridge between commitment complexes and U2 snRNP addition. *Genes Dev.*, **8**, 843–854.
18. Rutz,B. and Seraphin,B. (1999) Transient interaction of BBP/ScF1 and Mud2 with the splicing machinery affects the kinetics of spliceosome assembly. *RNA*, **5**, 819–831.

19. Nakagawa,T. and Ogawa,H. (1997) Involvement of the *MRE2* gene of yeast in formation of meiosis-specific double-strand breaks and crossover recombination through RNA splicing. *Genes Cells*, **2**, 65–79.
20. Spingola,M. and Ares,M. (2000) A yeast intronic splicing enhancer and Nam8p are required for Mer1p-activated splicing. *Mol. Cell*, **6**, 329–338.
21. Spingola,M., Armisen,J. and Ares,M. (2004) Mer1p is a modular splicing factors whose function depends on the conserved U2 snRNP protein Snu17p. *Nucleic Acids Res.*, **32**, 1242–1250.
22. Scherrer,F.W. and Spingola,M. (2006) A subset of Mer1p-dependent introns requires Bud13p for splicing activation and nuclear retention. *RNA*, **12**, 1361–1372.
23. Engebrecht,J., Voelkel-Meiman,K. and Roeder,G.S. (1991) Meiosis-specific RNA splicing in yeast. *Cell*, **66**, 1257–1268.
24. Cooper,K.F., Mallory,M.J., Egeland,D.B., Jarnik,M. and Strich,R. (2000) Ama1p is a meiosis-specific regulator of the anaphase promoting complex/cyclosome in yeast. *Proc. Natl Acad. Sci. USA*, **97**, 14548–14553.
25. Munding,E.M., Igel,A.H., Shiue,L., Dorighi,K.M., Trevino,L.R. and Ares,M. (2010) Integration of a splicing network within the meiotic gene expression program of *Saccharomyces cerevisiae*. *Genes Dev.*, **24**, 2693–2704.
26. Engebrecht,J. and Roeder,G.S. (1990) *MER1*, a yeast gene required for chromosome pairing and genetic recombination is induced in meiosis. *Mol. Cell. Biol.*, **10**, 2379–2389.
27. Nandabalan,K., Price,L. and Roeder,G.S. (1993) Mutations in U1 snRNA bypass the requirement for a cell type-specific RNA splicing factor. *Cell*, **73**, 407–415.
28. Nandabalan,K. and Roeder,G.S. (1995) Binding of a cell type-specific RNA splicing factor to its target regulatory sequence. *Mol. Cell. Biol.*, **15**, 1953–1960.
29. Enyenihi,A.H. and Saunders,W.S. (2003) Large-scale functional genomic analysis of sporulation and meiosis in *Saccharomyces cerevisiae*. *Genetics*, **163**, 47–54.
30. Malone,R.E., Pittman,D.L. and Nau,J.J. (1997) Examination of the intron in the meiosis-specific recombination gene *REC114* in *Saccharomyces*. *Mol. Gen. Genet.*, **255**, 410–419.
31. Leu,J.Y. and Roeder,G.S. (1999) Splicing of the meiosis-specific *HOP2* transcript utilizes a unique 5′ splice site. *Mol. Cell. Biol.*, **19**, 7933–7943.
32. Davis,C.A., Grate,L., Spingola,M. and Ares,M. (2000) Test of intron predictions reveals novel splice sites, alternatively spliced mRNAs and new introns in meiotically regulated genes of yeast. *Nucleic Acids Res.*, **28**, 1700–1706.
33. Rodriguez-Navarro,S., Igual,J.C. and Perez-Ortin,L.E. (2002) *SRC1*: a intron-containing yeast gene involved in sister chromatid segregation. *Yeast*, **19**, 43–54.
34. Juneau,K., Palm,C., Miranda,M. and Davis,R.W. (2007) High-density yeast-tiling array reveals previously undiscovered introns and extensive regulation of meiotic splicing. *Proc. Natl Acad. Sci. USA*, **104**, 1522–1527.
35. Monecke,T., Dickmanns,A. and Ficner,R. (2009) Structural basis for m^{7}G-cap hypermethylation of small nuclear, small nucleolar and telomerase RNA by the dimethyltransferase TGS1. *Nucleic Acids Res.*, **37**, 3865–3877.
36. Primig,M., Williams,R.M., Winzeler,E.A., Tevzadze,G.G., Conway,A.R., Hwang,S.Y., Davis,R.W. and Esposito,R.E. (2000) The core meiotic transcriptome in budding yeast. *Nature Genet.*, **26**, 415–423.
37. Rabitsch,K.P., Toth,A., Galova,M., Schleiffer,A., Schaffner,G., Aigner,E., Rupp,C., Penkner,A.M., Moreno-Borchart,A.C., Primig,M. *et al.* (2001) A screen for genes required for meiosis and spore formation based on whole-genome expression. *Curr. Biol.*, **11**, 1001–1009.
38. Spingola,M., Grate,L., Haussler,D. and Ares,M. (1999) Genome-wide bioinformatic and molecular analysis of introns in *Saccharomyces cerevisiae*. *RNA*, **5**, 221–234.
39. Warf,M.B. and Berglund,J.A. (2010) Role of RNA structure in regulating pre-mRNA splicing. *Trends Biochem. Sci.*, **35**, 169–178.
40. Zuker,M. (2003) Mfold web server for nucleic acid folding and hybridization prediction. *Nucleic Acids Res.*, **31**, 3406–3415.
41. Wang,Q., Zhang,L., Lynn,B. and Rymond,B.C. (2008) A BBP-Mud2p heterodimer mediates branchpoint recognition and influences splicing substrate abundance in budding yeast. *Nucleic Acids Res.*, **36**, 2787–2798.
42. Ansari,A. and Schwer,B. (1995) SLU7 and a novel activity, SSF1, act during the PRP16-dependent step of yeast pre-mRNA splicing. *EMBO J.*, **15**, 4001–4009.
43. Simoes-Barbosa,A., Meloni,D., Wohlschlegel,J.A., Konarska,M.M. and Johnson,P.J. (2008) Spliceosomal snRNAs in the unicellular eukaryote *Trichomonas vaginalis* are structurally conserved but lack a 5′-cap structure. *RNA*, **14**, 1617–1631.
44. Wersig,C. and Bindereif,A. (1992) Reconstitution of functional mammalian U4 small nuclear ribonucleoprotein: Sm protein binding is not essential for splicing in vitro. *Mol. Cell. Biol.*, **12**, 1460–1468.
45. Ségault,V., Will,C.L., Sproat,B.S. and Lührmann,R. (1995) In vitro reconstitution of mammalian U2 and U5 snRNPs active in splicing: Sm proteins are functionally interchangeable and are essential for the formation of functional U2 and U5 snRNPs. *EMBO J.*, **14**, 4010–4021.
46. Will,C.L., Rümpler,S., Gunnewiek,J.K., van Venrooij,W.J. and Lührmann,R. (1996) In vitro reconstitution of mammalian U1 snRNPs active in splicing: the U1-C protein enhances the formation of early (E) spliceosomal complexes. *Nucleic Acids Res.*, **24**, 4614–4623.
47. Dönmez,G., Hartmuth,K. and Lührmann,R. (2004) Modified nucleotides at the 5′ end of human U2 snRNA are required for spliceosomal E-complex formation. *RNA*, **10**, 1925–1933.
48. Yu,Y.T., Shu,M.D. and Steitz,J.A. (1998) Modifications of U2 snRNA are required for snRNP assembly and pre-mRNA splicing. *EMBO J.*, **17**, 5783–5795.
49. McKee,A.H.Z. and Kleckner,N. (1997) Mutations in *Saccharomyces cerevisiae* that block meiotic prophase chromosome metabolism and confer cell cycle arrest at pachytene identify two new meiosis-specific genes *SAE1* and *SAE3*. *Genetics*, **146**, 817–834.
50. San-Segundo,P.A. and Roeder,G.S. (1999) Pch2 links chromatin silencing to meiotic checkpoint control. *Cell*, **97**, 313–324.
51. Yedavalli,V. and Jeang,K.T. (2010) Trimethylguanosine capping selectively promotes expression of Rev-dependent HIV-1 RNAs. *Proc. Natl Acad. Sci. USA*, **107**, 14787–14792.